Korean J Physiol Pharmacol 2022;26(3):165-174
https://doi.org/10.4196/kjpp.2022.26.3.165

KJPP

Original Article

Oxymatrine inhibits the pyroptosis in rat insulinoma cells by affecting nuclear factor kappa B and nuclear factor (erythroid-derived 2)-like 2 protein/heme oxygenase-1 pathways

Jingying Gao[1,2,*], Lixia Xia[1], and Yuanyuan Wei[1,2]

[1]*Department of Pediatrics, Shanxi Medical University,* [2]*Pediatric Internal Medicine, Children's Hospital of Shanxi Province, Shanxi Medical University, Taiyuan 030001, China*

ARTICLE INFO

Received April 19, 2021
Revised January 11, 2022
Accepted February 4, 2022

***Correspondence**
Jingying Gao
E-mail: 13633513158@163.com

Key Words
Heme oxygenase-1
Nuclear factor (erythroid-derived 2)-like 2 protein
Nuclear factor kappa B
Oxymatrine
Pyroptosis

ABSTRACT As the mechanism underlying glucose metabolism regulation by oxymatrine is unclear, this study investigated the effects of oxymatrine on pyroptosis in INS-1 cells. Flow cytometry was employed to examine cell pyroptosis and reactive oxygen species (ROS) production. Cell pyroptosis was also investigated *via* transmission electron microscopy and lactate dehydrogenase (LDH) release. Protein levels were detected using western blotting and interleukin (IL)-1β and IL-18 secretion by enzyme-linked immunosorbent assay. The caspase-1 activity and DNA-binding activity of nuclear factor kappa B (NF-κB) and nuclear factor (erythroid-derived 2)-like 2 protein (Nrf2) were also assessed. In the high glucose and high fat-treated INS-1 cells (HG + PA), the caspase-1 activity and LDH content, as well as Nod-like receptor family pyrin domain containing 3, Gsdmd-N, caspase-1, apoptosis-associated speck-like protein containing a CARD, IL-1β, and IL-18 levels were increased. Moreover, P65 protein levels increased in the nucleus but decreased in the cytoplasm. Oxymatrine attenuated these effects and suppressed high glucose and high fat-induced ROS production. The increased levels of nuclear Nrf2 and heme oxygenase-1 (HO-1) in the HG + PA cells were further elevated after oxymatrine treatment, whereas cytoplasmic Nrf2 and Keleh-like ECH-associated protein levels decreased. Additionally, the elevated transcriptional activity of p65 in HG + PA cells was reduced by oxymatrine, whereas that of Nrf2 increased. The results indicate that the inhibition of pyroptosis in INS-1 cells by oxymatrine, a key factor in its glucose metabolism regulation, involves the suppression of the NF-κB pathway and activation of the Nrf2/HO-1 pathway.

INTRODUCTION

The main pathobiology of diabetes involves the decreased number and dysfunction of islet cells [1,2]. Inflammatory damage mediated by cytokines affects insulin secretion and the survival of islet cells [3,4]. Abnormal activation of Nod-like receptor family pyrin domain containing 3 (NLRP3) induces cell pyroptosis [5].

Pyroptosis is a programmed cell death mediated by various injury stimuli *via* inflammasome complexes. As a receptor receiving injury stimuli, NLRP3 plays an important role. The NLRP3 inflammasome is composed of NLRP3, apoptosis-associated speck-like protein containing a CARD (ASC) and cysteine aspartic acid-specific proteinase-1 (caspase-1). Activated inflammasomes stimulate caspase-1, which cleaves interleukin (IL)-1 and IL-18 precursor molecules, releasing IL-1 and IL-18, which participate in the inflammatory response [5,6]. Gasdermin D (Gsdmd) protein, the direct executor of cell pyroptosis, is cleaved into Gsdmd-N and Gsdmd-C by activated caspases. Gsdmd-N

Author contributions: J.G., L.X. and Y.W. obtained, analyzed and/or interpreted the data. J.G. and L.X. drafted the manuscript. Y.W. helped revise the manuscript.

has lipophilicity and pore-forming activity, which combines cell membrane lipids, induces cell membrane perforation, and releases inflammatory mediators [7].

Studies have found that high glucose, high fat, reactive oxygen species (ROS), and nuclear factor kappa B (NF-κB) can activate NLRP3 inflammasome and impair islet function [8-10]. ROS can damage islet β cells and inhibit insulin synthesis and secretion [11]. Nuclear factor (erythroid-derived 2)-like 2 protein (Nrf2) is a redox-sensitive transcription factor. Activated Nrf2 regulates downstream gene transcription to enhance the production of proteins, such as NAD (P)H: quinone oxidoreductase 1, glutamate-cysteine ligase, heme oxygenase-1 (HO-1), and superoxide dismutase, which reduce ROS production and ameliorate cell function disorders [12]. Nrf2 mainly mediates Keleh-like ECH-associated protein (Keap1)-Nrf2/antioxidant response element (ARE) signaling pathway. Under normal physiological conditions, Nrf2 is primarily negatively regulated by Keap1. Nrf2 bound to Keap1 remains in the cytoplasm, maintaining low transcriptional activity [13]. Under oxidative stress, Nrf2 is released from Keap1, translocates to the nucleus, and binds to the ARE to activate target gene transcription and produce antioxidant enzymes [14]. The number and activity of β cells have been found to be significantly lower in *Nrf2* knockout mice than in wild-type mice [15]. Yagishita *et al*. [16] have also demonstrated that Nrf2 expression can inhibit ROS accumulation in pancreatic β cells.

Oxymatrine is the main component of a traditional Chinese herb, *Sophora flavescens* Ait. Recent studies have demonstrated that oxymatrine is helpful for the treatment of diabetes. In umbilical vein endothelial cells, oxymatrine alleviates high glucose-induced endothelial toxicity by inhibiting ROS production [17,18]. Oxymatrine can reduce the levels of advanced glycation end products, ROS, and inflammatory cytokines in the kidney of diabetic rats [19]. We had previously shown that oxymatrine stimulated insulin secretion in isolated rat islets, increased rat insulinoma (INS-1) cell vitality and cell proliferation, and inhibited apoptosis in INS-1 cells [20]. However, as the role of oxymatrine in pyroptosis in INS-1 cells is unclear, we investigated the effects of oxymatrine on pyroptosis in INS-1 cells as well as the NF-κB pathway, ROS production, and levels of Nrf2 and HO-1.

METHODS

Cell cultures

The INS-1 cell line was obtained from AiYan Biological technology Co., Ltd. (Shanghai, China). The cells were cultured in RPMI-1640 medium (Gibco, Grand Island, NY, USA) supplemented with streptomycin (100 μg/ml; Sigma-Aldrich, St. Louis, MO, USA), penicillin (100 U/ml; Sigma-Aldrich), β-mercaptoethanol (50 μM; Gibco), sodium pyruvate (0.11 g/L; Sangon Biotech Co., Ltd., Shanghai, China), and fetal bovine serum (10%; Gibco) at 37°C in a humidified atmosphere containing 5% CO_2. The INS-1 cells were treated as follows: a control group: no treatment; HG + PA group: high glucose (30 mM glucose [Sangon Biotech Co., Ltd.]) + high fat (400 μM palmitic acid sodium [Sigma-Aldrich]); HG + PA + oxymatrine (1 μM) group: high glucose (30 mM glucose) + high fat (400 μM palmitic acid sodium) + oxymatrine (1 μM [Sigma-Aldrich]); HG + PA + oxymatrine (10 μM) group: high glucose (30 mM glucose) + high fat (400 μM palmitic acid sodium) + oxymatrine (10 μM). The concentrations of oxymatrine were based on the results of our previous work [20].

Flow cytometry analysis

The FAM-FLICA Caspase-1 Assay Kit (Immuno Chemistry Technologies, Bloomington, MN, USA) was employed for cell pyroptosis detection. The INS-1 cells were seeded in 6-well plates at a density of 4×10^5 cells/ml. After treatment for 24 h, the cells were collected, washed, and centrifuged (1,000 rpm, 5 min). The supernatant was discarded, and the pellets were mixed with FAM-FLICA caspase-1 (10 μl:290 μl) and incubated at 37°C for 1 h. After the medium was removed by centrifugation and the samples washed three times with 1 × Apoptosis wash buffer, a working solution of propidium iodide (100 μg/ml) was added to the cell suspension (1 μl:100 μl). The cells were incubated at room temperature for 15 min and detected using a Beckman DxFLEX flow cytometer (Beckman Coulter, Inc., Indianapolis, IN, USA).

Reactive oxygen species assay

A Reactive Oxygen Species Assay Kit (Beyotime Biotechnology, Shanghai, China) was used to measure ROS production. After treatment for 24 h, the INS-1 cells were digested with trypsin without EDTA (Gibco), centrifuged (1,500 rpm, 5 min) at 4°C, and collected. Each sample was incubated with 1.5 ml of a working solution of dichlorodihydrofluorescein diacetate (5 μM) at 37°C in the dark for 20 min. Subsequently, the cells were centrifuged (1,500 rpm, 10 min), and the staining solution was carefully discarded. After washing two times with phosphate-buffered saline (PBS), the cells were resuspended with PBS (200 μl/well). Beckman DxFLEX flow cytometer was used to detect the fluorescence signals of 10,000 cells within half an hour to obtain a curve.

Lactate dehydrogenase (LDH) release assay

The release of LDH in the supernatants was measured by using a commercially available LDH assay kit (Jiancheng Bioengineering Institute, Nanjing, China) according to the manufacturer's instructions. The INS-1 cells were treated as follows: control; HG + PA; HG + PA + oxymatrine (1 μM); HG + PA + oxymatrine (10 μM). The cells were cultured in a 24-well plate for 24 h. The absorbance was determined using a multifunctional microplate reader (Berthold Technologies, Bad Wildbad, Germany) at 450 nm.

Transmission electron microscopy (TEM)

The INS-1 cells were treated as follows: control; HG + PA; HG + PA + oxymatrine (10 μM). After the cells were digested and centrifuged twice (1,000 rpm, 5 min, and 1,600 rpm, 5 min), the supernatant was removed and the cell masses collected. The samples were fixed (2.5% glutaraldehyde and 1% osmic acid), dehydrated (ethanol and acetone), embedded in epoxy resin, sectioned using a microtome to a thickness of 50 nm, and stained (uranium acetate and lead citrate). Finally, the specimens were observed and images acquired using a transmission electron microscope (TEM; Hitachi, Tokyo, Japan).

Enzyme-linked immunosorbent assay (ELISA) to measure IL-1β and IL-18 secretion

IL-1β and IL-18 concentrations were measured using an IL-1β ELISA kit (R&D Systems, Minneapolis, MN, USA) and an IL-18 ELISA kit (Huijia Biological Technology Co., Ltd., Xiamen, China), respectively. The INS-1 cells were treated as follows: control; HG + PA; HG + PA + oxymatrine (10 μM). The cells were seeded in 96-well plates (5×10^3 cells/well) for 24 h. After the cells were digested and centrifuged (2,000 rpm, 20 min), the supernatant was collected, and the assay performed according to the manufacturer's instructions. The optical density was determined at 450 nm by using the multifunctional microplate reader.

Measurement of caspase-1 activity

Caspase-1 activity was assessed by using a caspase-1 activity assay kit (Beyotime Biotechnology) according to the manufacturer's instructions. The INS-1 cells were treated as follows: control; HG + PA; HG + PA + oxymatrine (10 μM). The cells were incubated in 96-well plates (5×10^3 cells/well) for 24 h. After the cells were digested and centrifuged (700 rpm, 5 min, 4°C), the supernatant was discarded. Subsequently, the cells were resuspended with pyrolysis buffer (100 μl pyrolysis buffer for 2×10^6 cells), lysed in an ice bath for 15 min, and centrifuged (3,800 rpm, 10 min, 4°C). The supernatant was mixed with precooled Ac-YVAD-pNA (2 mM) and incubated at 37°C for 60 min. The absorbance was measured at a wavelength of 405 nm using the multifunctional microplate reader.

Western blotting

The protein levels were analyzed by western blotting. The INS-1 cells were treated as follows: control; HG + PA; HG + PA + oxymatrine (1 μM); HG + PA + oxymatrine (10 μM). The cells were cultured in 6-well plates (4×10^5 cells/ml) for 24 h. In brief, the cell lysates were electrophoresed and transferred onto polyvinylidene fluoride membranes. Then, the membranes were incubated with the following primary antibodies (diluted in Tris-buffered saline with 0.1% Tween-20 [TBST] buffer): anti-NLRP3 antibody (ab214185, 1:1,000), anti-IL-1β antibody (ab205924, 1:1,000), anti-NF-κB p65 antibody (ab16502, 1:2,000), anti-Nrf2 antibody (ab89443, 1:500), anti-HO-1 antibody (ab13243, 1:2,000), anti-Keap1 antibody (ab119403, 1:1,000), anti-ASC antibody (ab180799, 1:2,000), and β-actin antibody (ab8226, 1:1,000) from Abcam (Cambridge, UK); anti-Gsdmd antibody (93709, 1:1,000) and anti-Histone H3 antibody (4499, 1:2,000) from Cell Signaling Technology (Boston, MA, USA); and anti-caspase-1 antibody (NBP1-45433, 1:1,000) from Novus Biologicals (Littleton, CO, USA). After washing, the membranes were incubated with the appropriate secondary antibody (diluted in TBST buffer) from Abcam (1:5,000, Cambridge, UK). Image Pro Plus 6.0 software (Media Cybernetics, Houston, TX, USA) was used to determine the intensity of the protein bands.

Luciferase reporter gene assay for DNA-binding activity of NF-κB and Nrf2

A firefly luciferase reporter gene assay kit was obtained from Beyotime Biotechnology. The NF-κB-luc reporter plasmid and Nrf2-luc reporter plasmid were purchased from Genomeditech (Shanghai, China). The INS-1 cells were treated as follows: control; HG + PA; HG + PA + oxymatrine (10 μM). After 36–48 h of co-transfection with the plasmids, the cells in each well were treated with 100 μl of pyrolysis buffer and centrifuged (3,700 rpm, 3 min). Then, the supernatant was collected and mixed with luciferase test reagent (100 μl sample:100 μl luciferase test reagent) to measure the relative luciferase activity using the multifunctional microplate reader. The measurement time was 10 sec and the interval was 2 sec.

Statistical analysis

The data were expressed as mean ± standard deviation (SD). Sigmaplot (Systat Software, San Jose, CA, USA) was used to statistical analysis. Statistical differences were tested by one-way analysis of variance (ANOVA) and Tukey's test. $p < 0.05$ was considered significant.

RESULTS

Oxymatrine protected INS-1 cells from pyroptosis

Flow cytometry, the LDH release assay, and TEM were employed to determine the effects of oxymatrine on pyroptosis in INS-1 cells. As shown in Fig. 1, mitochondrial cristae and abundant organelles were visible in the control cells; no mitochondrial swelling or vacuolar degeneration was observed. The number of autophagosomal vesicles was higher in the HG + PA cells, which also showed mitochondrial swelling, vacuolar degeneration, ir-

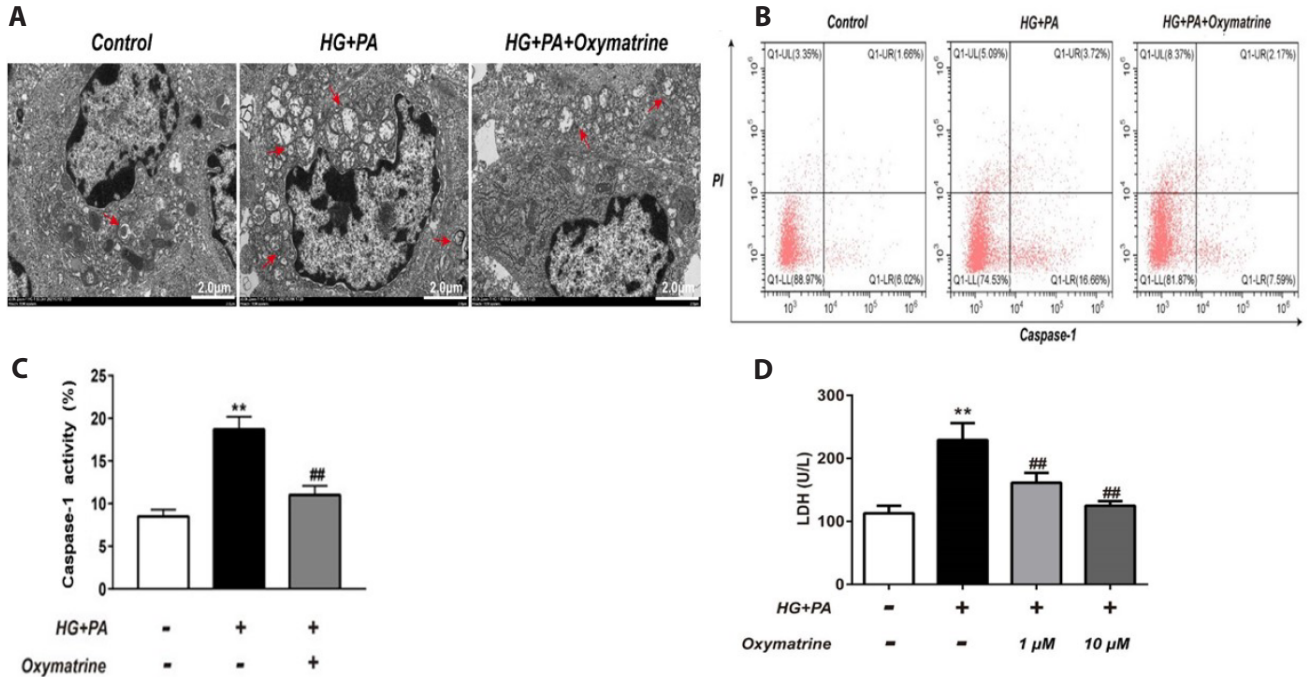

Fig. 1. Oxymatrine protected INS-1 cells from pyroptosis. (A) The electron microscopic analysis of different cells. Scale bar: 2 μm; Oxymatrine: 10 μM. (B) Representative graphics from flow cytometry analysis were showed; Oxymatrine: 10 μM. (C) The caspase-1 activity analysis of different cells; Oxymatrine: 10 μM. (D) The LDH release analysis of different cells. control: no treatment; HG: high glucose (30 mM glucose); PA: palmitic acid sodium (400 μM). Arrows: the autophagosomal vesicles. Data are presented as mean ± SD and represent an average of three experiments. LDH, lactate dehydrogenase. **p < 0.01 *vs*. control, ##p < 0.01 *vs*. HG + PA; the experiments were repeated three times.

regular nuclear morphology, local nuclear membrane depression, decreased organelles, and a large number of intracellular vacuoles (Fig. 1A). The HG + PA cells showed an increase in caspase-1 activity to 18.70% ± 1.48% at 24 h (p < 0.01 *vs*. control, Fig. 1B, C) and the LDH content (p < 0.01 *vs*. control, Fig. 1D). Incubation of the HG + PA cells with oxymatrine (10 μM) decreased the number of autophagosomal vesicles in the cytoplasm (Fig. 1A) and caspase-1 activity (11.00% ± 1.08% at 24 h; p < 0.01 *vs*. HG + PA, Fig. 1B, C). Oxymatrine (1 μM and 10 μM) also suppressed LDH release (p < 0.01 *vs*. HG + PA, Fig. 1D).

Oxymatrine decreased the levels of NLRP3, Gsdmd-N, caspase-1, ASC, IL-1β, and IL-18 in INS-1 cells under high glucose and high fat conditions

After the cells were treated under different conditions, the levels of NLRP3, Gsdmd-N, caspase-1, ASC, and IL-1β were detected by Western blotting, while IL-1β and IL-18 secretion was measured using ELISA. Caspase-1 activity was examined by spectrophotometry. The levels of NLRP3, Gsdmd-N, caspase-1, IL-1β, and ASC (p < 0.01 *vs*. control, Fig. 2A–G), the secretion of IL-1β and IL-18 (p < 0.01 *vs*. control, Fig. 2H), and caspase-1 activity (p < 0.01 *vs*. control, Fig. 2I) were increased in HG + PA cells. As expected, treatment with oxymatrine decreased these protein levels (p < 0.01 *vs*. HG + PA, Fig. 2B–E; p < 0.05 *vs*. HG + PA, Fig. 2D, G), the secretion of IL-1β and IL-18 (p < 0.01 *vs*. HG + PA, Fig. 2H), and caspase-1 activity (p < 0.01 *vs*. HG + PA, Fig. 2I).

Oxymatrine inhibited high glucose and high fat-induced ROS production in INS-1 cells

As indicated in Fig. 3, ROS production was higher in HG + PA cells than in the control cells (p < 0.01 *vs*. control). Treatment with oxymatrine suppressed ROS production in HG + PA cells (p < 0.05 *vs*. HG + PA, Fig. 3A, B).

Oxymatrine affected NF-κB (p65) levels in INS-1 cells at different times

Treatment of INS-1 cells under different conditions for 0.5 h, 1 h, or 2 h altered NF-κB (p65) protein levels. In HG + PA cells, the nuclear p65 protein levels increased over time (0.5 h: 2.32 ± 0.22; 1 h: 3.64 ± 0.32; 2 h: 3.99 ± 0.35) (p < 0.01 *vs*. control, Fig. 4A, B, D, F) but decreased after treatment with oxymatrine (0.5 h: 1.17 ± 0.14; 1 h: 1.41 ± 0.14; 2 h: 1.82 ± 0.12) (p < 0.01 *vs*. HG + PA, Fig. 4A, B, D, F). Compared with the control cells, cytoplasmic p65 protein levels of HG + PA cells decreased over time (0.5 h: 0.54 ± 0.05; 1 h: 0.40 ± 0.05; 2 h: 0.34 ± 0.03) (p < 0.01 *vs*. control, Fig. 4A, C, E, G) but increased after treatment with oxymatrine (0.5 h: 0.91 ± 0.07; 1 h: 0.77 ± 0.08; 2 h: 0.66 ± 0.06) (p < 0.01 *vs*. HG + PA, Fig. 4A, C, E, G).

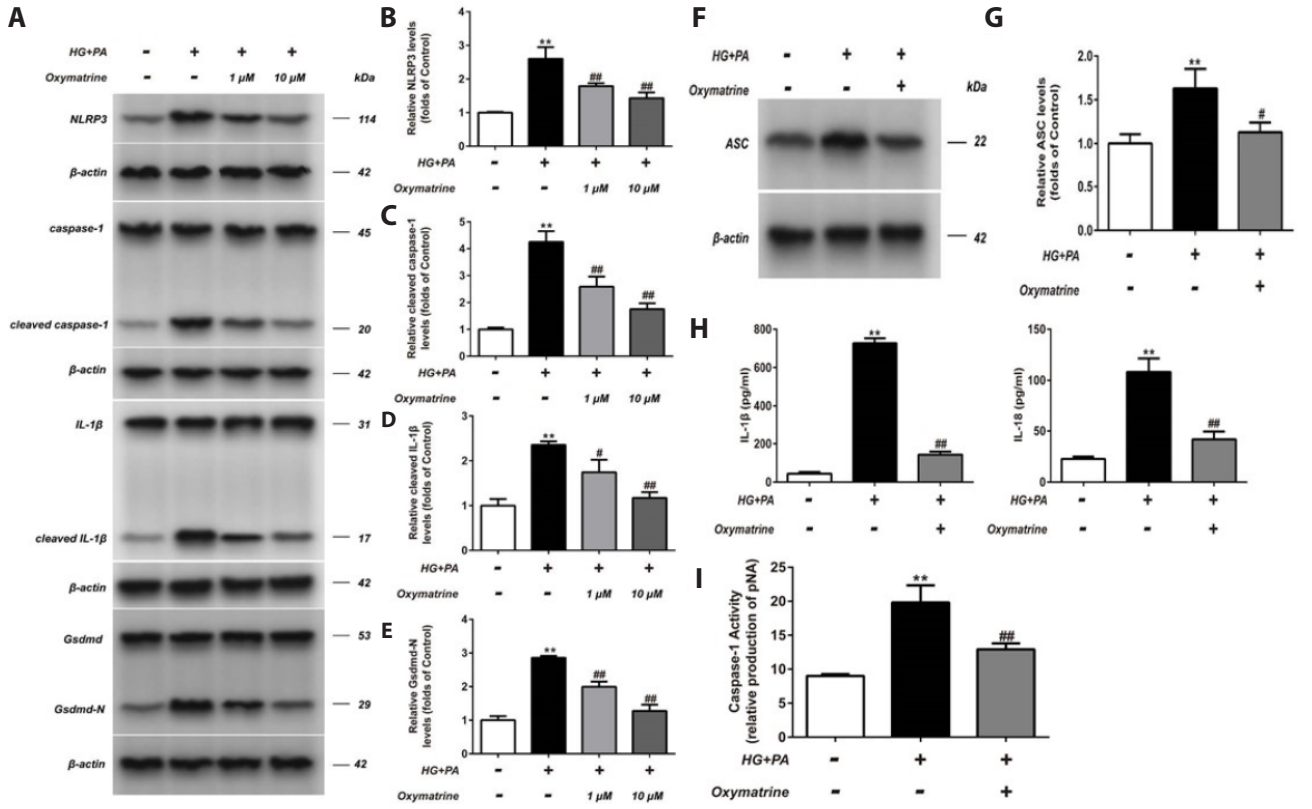

Fig. 2. Oxymatrine decreased the levels of NLRP3, Gsdmd-N, caspase-1, ASC, IL-1β, and IL-18 in INS-1 cells under high glucose and high fat conditions. (A) Representative Western blotting bands of NLRP3, Gsdmd-N, caspase-1, and IL-1β proteins were showed. (B) Analysis of the amount of NLRP3 proteins. (C) Analysis of the amount of caspase-1 proteins. (D) Analysis of the amount of IL-1β proteins. (E) Analysis of the amount of Gsdmd-N proteins. (F) Representative western blotting bands of ASC proteins were showed; Oxymatrine: 10 μM. (G) Analysis of the amount of ASC proteins; Oxymatrine: 10 μM. (H) Analysis of the secretion of IL-1β and IL-18; Oxymatrine: 10 μM. (I) Analysis of the activity of caspase-1; Oxymatrine: 10 μM. control: no treatment; HG: high glucose (30 mM glucose); PA: palmitic acid sodium (400 μM). Data are presented as mean ± SD and represent an average of three experiments. NLRP3, Nod-like receptor family pyrin domain containing 3; Gsdmd, Gasdermin D; caspase-1, cysteine aspartic acid-specific proteinase-1; ASC, apoptosis-associated speck-like protein containing a CARD; IL, interleukin. Data from Western blotting are normalized to control. **p < 0.01 *vs*. control, #p < 0.05, ##p < 0.01 *vs*. HG + PA; the experiments were repeated three times.

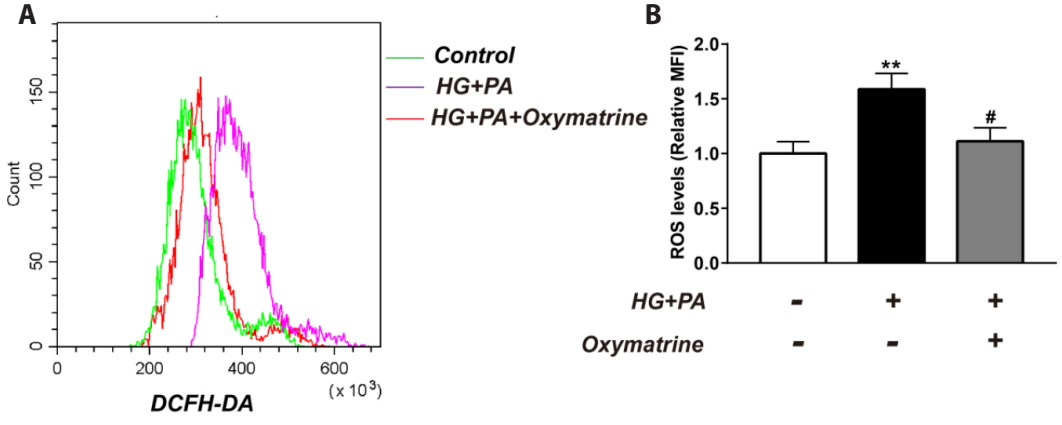

Fig. 3. Oxymatrine inhibited high glucose and high fat-induced ROS production in INS-1 cells. (A) Representative graphics of ROS production were showed. (B) The ROS production from different cells. control: no treatment; HG: high glucose (30 mM glucose); PA: palmitic acid sodium (400 μM); Oxymatrine: 10 μM. Data are presented as mean ± SD and represent an average of three experiments. ROS, reactive oxygen species; DCFH-DA, Dichloro-dihydro-fluorescein diacetate; MFI, mean fluorescence intensity. Data are normalized to control. **p < 0.01 *vs*. control, #p < 0.05 *vs*. HG + PA; the experiments were repeated three times.

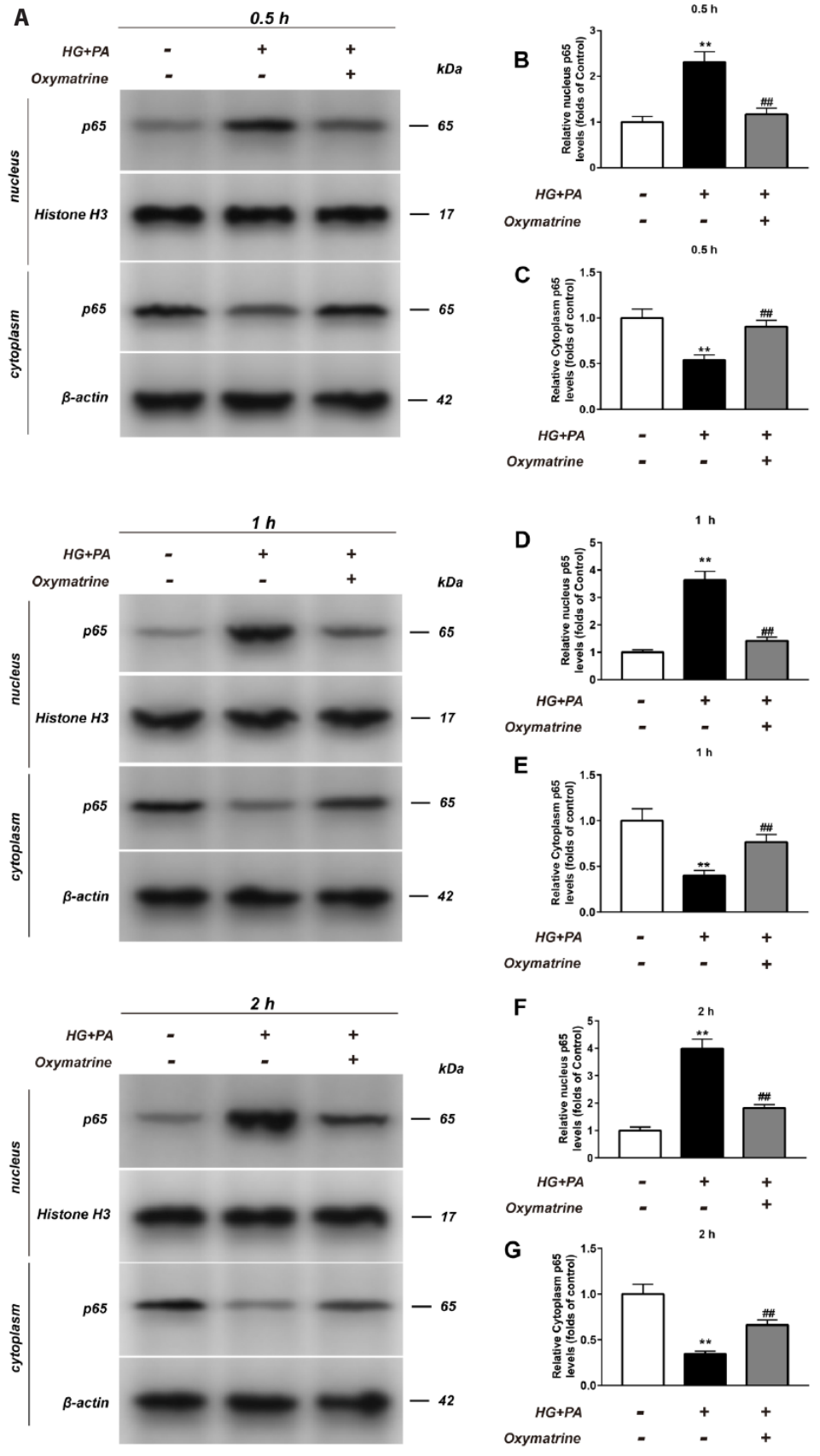

Fig. 4. Oxymatrine affected NF-κB (p65) levels in INS-1 cells at different times. (A) Representative Western blotting bands of p65 proteins in the nucleus or cytoplasm were showed. (B) Analysis of the amount of p65 proteins in the nucleus when the cells were incubated for 0.5 h. (C) Analysis of the amount of p65 proteins in the cytoplasm when the cells were incubated for 0.5 h. (D) Analysis of the amount of p65 proteins in the nucleus when the cells were incubated for 1 h. (E) Analysis of the amount of p65 proteins in the cytoplasm when the cells were incubated for 1 h. (F) Analysis of the amount of p65 proteins in the nucleus when the cells were incubated for 2 h. (G) Analysis of the amount of p65 proteins in the cytoplasm when the cells were incubated for 2 h. Control: no treatment; HG: high glucose (30 mM glucose); PA: palmitic acid sodium (400 μM); Oxymatrine: 10 μM. Data are presented as mean ± SD and represent an average of three experiments. NF-κB, nuclear factor kappa B. Data are normalized to control. $^{**}p < 0.01$ *vs*. control, $^{\#\#}p < 0.01$ *vs*. HG + PA; the experiments were repeated three times.

https://doi.org/10.4196/kjpp.2022.26.3.165

Oxymatrine affected Nrf2, HO-1, and Keap1 levels in INS-1 cells

As shown in Fig. 5, the levels of HO-1 and nuclear Nrf2 proteins increased in HG + PA cells compared with those in the control cells ($p < 0.01$ *vs*. control, Fig. 5A, B; $p < 0.05$ *vs*. control, Fig. 5A, E). In contrast, levels of Keap1 and cytoplasmic Nrf2 proteins decreased in HG + PA cells ($p < 0.01$ *vs*. control, Fig. 5A, C, D). The treatment of HG + PA cells with oxymatrine increased nuclear Nrf2 and HO-1 levels ($p < 0.01$ *vs*. HG + PA, Fig. 5A, B, E) and decreased cytoplasmic Nrf2 and Keap1 levels ($p < 0.05$ *vs*. HG + PA, Fig. 5 A, C, D) to a greater extent.

Oxymatrine affected DNA-binding activity of NF-κB (p65) and Nrf2 in INS-1 cells

The DNA-binding activity of NF-κB (p65) and Nrf2 were assessed in INS-1 cells after 24 h treatment under different conditions. Compared with the control cells, the transcriptional activity of p65 and Nrf2 was activated in HG + PA cells ($p < 0.01$ *vs*. control, Fig. 6A, B). Oxymatrine treatment inhibited the transcriptional activity of p65 ($p < 0.05$ *vs*. HG + PA, Fig. 6A) but enhanced that of Nrf2 ($p < 0.01$ *vs*. HG + PA, Fig. 6B).

DISCUSSION

Previous reports have indicated that high glucose and high fat concentrations can induce cell pyroptosis. Li *et al*. [21] have shown that high glucose-treated hippocampal neuronal cells undergo pyroptosis *in vitro* in an NLRP3-dependent manner. Gu *et al*. [22] demonstrated that high glucose levels trigger pyroptosis in human renal glomerular endothelial cells. In high fat diet-fed obese mice, hypertrophic adipocytes have been found to undergo pyroptosis [23]. In the mouse pre-osteoblast MC3T3-E1 cell line, high glucose inhibits the proliferation of osteoblasts by activating the pyroptosis pathway [24]. Pyroptosis is also implicated in the high glucose-induced cell death of H9c2 cardiomyocytes, human ventricular cardiomyocytes, and EA.hy926 endothelial cells [25-27]. Moreover, pyroptosis is closely related to diabetes. Type 2 diabetic db/db mice showed high levels of NLRP3 and IL-1β [28]. However, after the application of an NLRP3 inhibitor, these type 2 diabetic mice showed a decrease in NLRP3 and IL-1 β levels along with an amelioration of insulin resistance [28]. A 2013 report also confirms that type 2 diabetes mellitus (T2DM) is associated with the NLRP3-related inflammatory response, which is induced by activating the mitochondrial ROS pathway [29]. In T2DM rats, NLRP3 is activated by the NF-κB and thioredoxin interacting protein, which affects the progression of diabetic cardiomyopathy [25]. Pyroptosis is also commonly observed in various complications of T2DM, such as diabetic nephropathy and diabetic

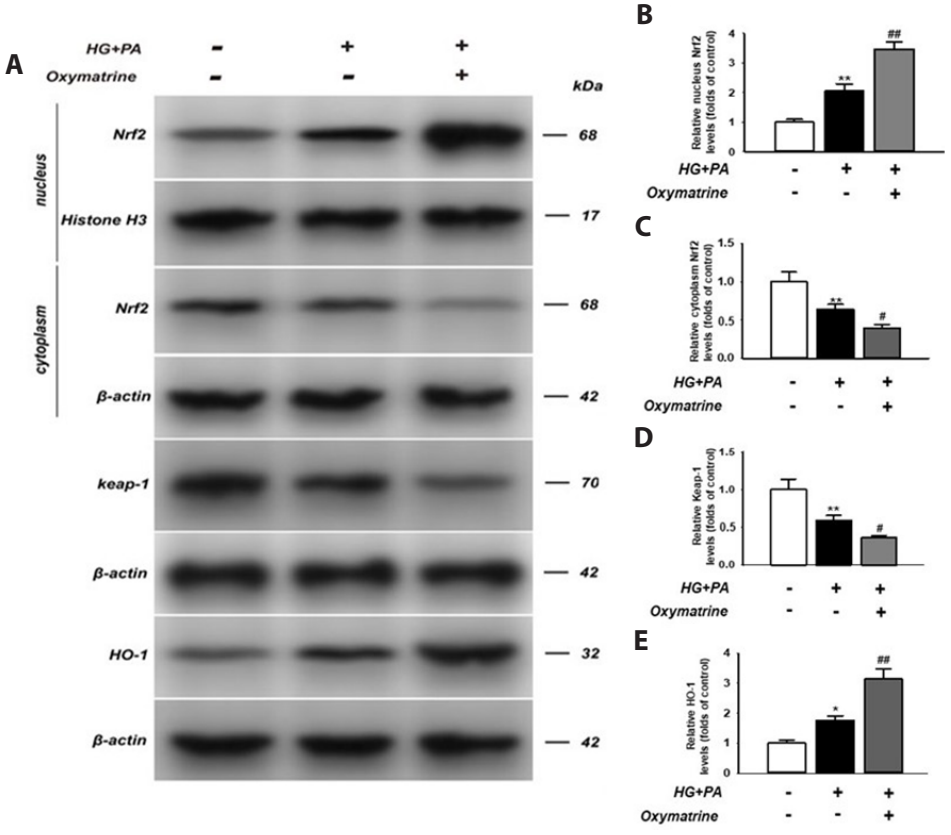

Fig. 5. Oxymatrine affected Nrf2, HO-1, and Keap1 levels in INS-1 cells. (A) Representative Western blotting bands of Nrf2, HO-1, and Keap1 proteins in the nucleus or cytoplasm were showed. (B) Analysis of the amount of Nrf2 proteins in the nucleus. (C) Analysis of the amount of Nrf2 proteins in the cytoplasm. (D) Analysis of the amount of Keap1 proteins. (E) Analysis of the amount of HO-1 proteins. Control: no treatment; HG: high glucose (30 mM glucose); PA: palmitic acid sodium (400 μM); Oxymatrine: 10 μM. Data are presented as mean ± SD and represent an average of three experiments. Nrf2, nuclear factor (erythroid-derived 2)-like 2 protein; HO-1, heme oxygenase-1; Keap1, Keleh-like ECH-associated protein. Data are normalized to control. *$p < 0.05$ *vs*. control, **$p < 0.01$ *vs*. control, $^{\#}p < 0.05$ *vs*. HG + PA. $^{\#\#}p < 0.01$ *vs*. HG + PA; the experiments were repeated three times.

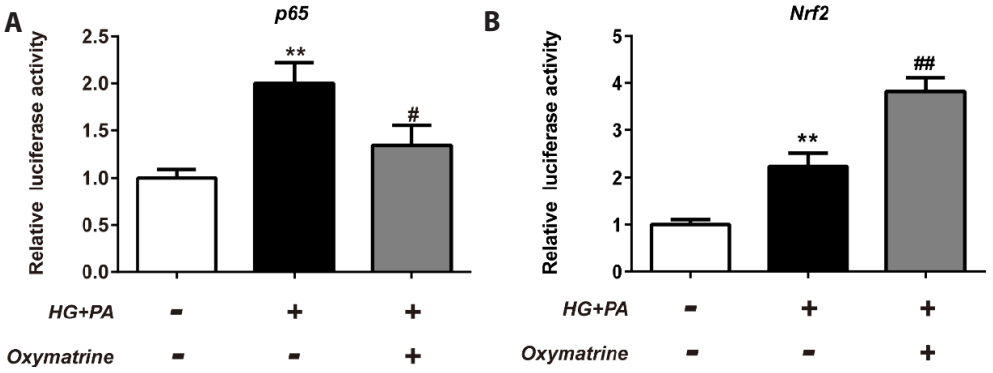

Fig. 6. Oxymatrine affected DNA-binding activity of NF-κB (p65) and Nrf2 in INS-1 cells. (A) Analysis of the DNA-binding activity of NF-κB (p65). (B) Analysis of the DNA-binding activity of Nrf2. Control: no treatment; HG: high glucose (30 mM glucose); PA: palmitic acid sodium (400 μM); Oxymatrine: 10 μM . Data are presented as mean ± SD and represent an average of three experiments. NF-κB, nuclear factor kappa B; Nrf2, nuclear factor (erythroid-derived 2)-like 2 protein. Data are normalized to control. **p < 0.01 *vs*. control, #p < 0.05, ## p < 0.01 *vs*. HG + PA; the experiments were repeated three times.

retinopathy [30,31]. Consistent with these findings, the present study data showed an increase in the number of autophagosomal vesicles in the cytoplasm of HG + PA INS-1 cells. High glucose and high fat also increased LDH release, caspase-1 activity, and the levels of related inflammatory factors, including NLRP3, IL-1β, IL-18, Gsdmd-N, caspase-1, and ASC, leading to pyroptosis in INS-1 cells. However, these changes were suppressed by oxymatrine treatment, demonstrating that oxymatrine can inhibit high glucose and high fat-induced pyroptotic cell death in INS-1 cells.

Hyperglycemia reduces the binding affinity of the NF-κB (p65) subunit to IκB alpha, causing increased nuclear translocation of p65 [32] and transcription of target genes involved in inflammatory responses [33]. Saturated fatty acids may also directly activate the toll-like-4 receptor, resulting in the activation of the downstream c-Jun NH 2-terminal kinase and inhibitor kappa B kinase β/NF-κB cascade [34,35]. Lipotoxicity, glucotoxicity, and glucolipotoxicity induce metabolic stress, which manifests as increased oxidative stress and ROS production [36-38]. As mentioned above, the activation of NLRP3 is affected by the NF-κB (p65) pathway and ROS production. Under oxidative stress, the transcriptional activity of Nrf2 was increased, and Nrf2 reduced ROS production by mediating the transcription and expression of a series of antioxidant stress proteins such as HO-1. Thus, both NF-κB and Nrf2 regulate NLRP3 by different mechanisms. Oxymatrine has been reported to regulate NF-κB pathway and Nrf2 expression. The NF-κB pathway is suppressed by oxymatrine in colon cancer cells and fibroblast-like synoviocytes [39,40]. By increasing the levels of Nrf2 and HO-1, oxymatrine reduces renal ischemia-reperfusion injury, cerebral ischemia-reperfusion injury, arsenic trioxide (As_2O_3)-affected liver injury, and lipopolysaccharide/D-galactosamine-induced acute liver failure [41-44]. Therefore, to explore the mechanism of oxymatrine-inhibited pyroptosis in INS-1 cells, we analyzed the effects of oxymatrine on these factors. The results showed that high glucose and high fat increased the DNA-binding activity of NF-κB (p65) and Nrf2. Treatment with oxymatrine suppressed the transcriptional activity of NF-κB and reduced the entry of P65 into the nucleus. In contrast, oxymatrine promoted *Nrf2* transcription, which increased HO-1 expression and reduced intracellular ROS levels.

In summary, oxymatrine inhibits NLRP3-mediated pyroptosis in INS-1 cells, which may be related to its inhibition of the NF-κB pathway and activation of the Nrf2 pathway. These results contribute to understanding the mechanism of oxymatrine-regulated islet cell function and provide a theoretical basis for the clinical application of oxymatrine for the treatment of diabetes.

FUNDING

This work was supported by grants from Youth Science Foundation of Shanxi Province (201801D221395), Startup Foundation for Doctors of Shanxi Medical University (BS03201640).

ACKNOWLEDGEMENTS

None.

CONFLICTS OF INTEREST

The authors declare no conflicts of interest.

REFERENCES

1. Brennan MA, Cookson BT. Salmonella induces macrophage death by caspase-1-dependent necrosis. *Mol Microbiol.* 2000;38:31-40.
2. Westwell-Roper C, Nackiewicz D, Dan M, Ehses JA. Toll-like receptors and NLRP3 as central regulators of pancreatic islet inflammation in type 2 diabetes. *Immunol Cell Biol.* 2014;92:314-323.
3. Donath MY, Böni-Schnetzler M, Ellingsgaard H, Ehses JA. Islet

inflammation impairs the pancreatic beta-cell in type 2 diabetes. *Physiology (Bethesda).* 2009;24:325-331.
4. Christensen CS, Christensen DP, Lundh M, Dahllöf MS, Haase TN, Velasquez JM, Laye MJ, Mandrup-Poulsen T, Solomon TP. Skeletal muscle to pancreatic β-cell cross-talk: the effect of humoral mediators liberated by muscle contraction and acute exercise on β-cell apoptosis. *J Clin Endocrinol Metab.* 2015;100:E1289-E1298. Erratum in: *J Clin Endocrinol Metab.* 2016;101:2265.
5. He WT, Wan H, Hu L, Chen P, Wang X, Huang Z, Yang ZH, Zhong CQ, Han J. Gasdermin D is an executor of pyroptosis and required for interleukin-1β secretion. *Cell Res.* 2015;25:1285-1298.
6. Schneider KS, Groß CJ, Dreier RF, Saller BS, Mishra R, Gorka O, Heilig R, Meunier E, Dick MS, Ćiković T, Sodenkamp J, Médard G, Naumann R, Ruland J, Kuster B, Broz P, Groß O. The inflammasome drives GSDMD-independent secondary pyroptosis and IL-1 release in the absence of caspase-1 protease activity. *Cell Rep.* 2017;21:3846-3859.
7. Chen X, He WT, Hu L, Li J, Fang Y, Wang X, Xu X, Wang Z, Huang K, Han J. Pyroptosis is driven by non-selective gasdermin-D pore and its morphology is different from MLKL channel-mediated necroptosis. *Cell Res.* 2016;26:1007-1020.
8. Masters SL, Latz E, O'Neill LA. The inflammasome in atherosclerosis and type 2 diabetes. *Sci Transl Med.* 2011;3:81ps17.
9. Vandanmagsar B, Youm YH, Ravussin A, Galgani JE, Stadler K, Mynatt RL, Ravussin E, Stephens JM, Dixit VD. The NLRP3 inflammasome instigates obesity-induced inflammation and insulin resistance. *Nat Med.* 2011;17:179-188.
10. Legrand-Poels S, Esser N, L'homme L, Scheen A, Paquot N, Piette J. Free fatty acids as modulators of the NLRP3 inflammasome in obesity/type 2 diabetes. *Biochem Pharmacol.* 2014;92:131-141.
11. Gerber PA, Rutter GA. The role of oxidative stress and hypoxia in pancreatic beta-cell dysfunction in diabetes mellitus. *Antioxid Redox Signal.* 2017;26:501-518.
12. Yates MS, Tran QT, Dolan PM, Osburn WO, Shin S, McCulloch CC, Silkworth JB, Taguchi K, Yamamoto M, Williams CR, Liby KT, Sporn MB, Sutter TR, Kensler TW. Genetic versus chemoprotective activation of Nrf2 signaling: overlapping yet distinct gene expression profiles between Keap1 knockout and triterpenoid-treated mice. *Carcinogenesis.* 2009;30:1024-1031.
13. Sun X, Ou Z, Chen R, Niu X, Chen D, Kang R, Tang D. Activation of the p62-Keap1-NRF2 pathway protects against ferroptosis in hepatocellular carcinoma cells. *Hepatology.* 2016;63:173-184.
14. Jaramillo MC, Zhang DD. The emerging role of the Nrf2-Keap1 signaling pathway in cancer. *Genes Dev.* 2013;27:2179-2191.
15. Li S, Vaziri ND, Masuda Y, Hajighasemi-Ossareh M, Robles L, Le A, Vo K, Chan JY, Foster CE, Stamos MJ, Ichii H. Pharmacological activation of Nrf2 pathway improves pancreatic islet isolation and transplantation. *Cell Transplant.* 2015;24:2273-2283.
16. Yagishita Y, Fukutomi T, Sugawara A, Kawamura H, Takahashi T, Pi J, Uruno A, Yamamoto M. Nrf2 protects pancreatic β-cells from oxidative and nitrosative stress in diabetic model mice. *Diabetes.* 2014;63:605-618.
17. Yi Y, Shen Y, Wu Q, Rao J, Guan S, Rao S, Huang L, Tan M, He L, Liu L, Li G, Liang S, Xiong W, Gao Y. Protective effects of oxymatrine on vascular endothelial cells from high-glucose-induced cytotoxicity by inhibiting the expression of A_{2B} receptor. *Cell Physiol Biochem.* 2018;45:558-571.
18. Wang L, Li X, Zhang Y, Huang Y, Zhang Y, Ma Q. Oxymatrine ameliorates diabetes-induced aortic endothelial dysfunction via the regulation of eNOS and NOX4. *J Cell Biochem.* 2018;120:7323-7332.
19. Guo C, Han F, Zhang C, Xiao W, Yang Z. Protective effects of oxymatrine on experimental diabetic nephropathy. *Planta Med.* 2014;80:269-276.
20. Gao J, Xia L, Wei Y. Voltage-gated potassium channels are involved in oxymatrine-regulated islet function in rat islet β cells and INS-1 cells. *Iran J Basic Med Sci.* 2021;24:460-468.
21. Li DX, Wang CN, Wang Y, Ye CL, Jiang L, Zhu XY, Liu YJ. NLRP3 inflammasome-dependent pyroptosis and apoptosis in hippocampus neurons mediates depressive-like behavior in diabetic mice. *Behav Brain Res.* 2020;391:112684.
22. Gu J, Huang W, Zhang W, Zhao T, Gao C, Gan W, Rao M, Chen Q, Guo M, Xu Y, Xu YH. Sodium butyrate alleviates high-glucose-induced renal glomerular endothelial cells damage via inhibiting pyroptosis. *Int Immunopharmacol.* 2019;75:105832.
23. Giordano A, Murano I, Mondini E, Perugini J, Smorlesi A, Severi I, Barazzoni R, Scherer PE, Cinti S. Obese adipocytes show ultrastructural features of stressed cells and die of pyroptosis. *J Lipid Res.* 2013;54:2423-2436.
24. Yang L, Liu J, Shan Q, Geng G, Shao P. High glucose inhibits proliferation and differentiation of osteoblast in alveolar bone by inducing pyroptosis. *Biochem Biophys Res Commun.* 2020;522:471-478. Erratum in: *Biochem Biophys Res Commun.* 2020;528:404.
25. Luo B, Li B, Wang W, Liu X, Xia Y, Zhang C, Zhang M, Zhang Y, An F. NLRP3 gene silencing ameliorates diabetic cardiomyopathy in a type 2 diabetes rat model. *PLoS One.* 2014;9:e104771.
26. Jeyabal P, Thandavarayan RA, Joladarashi D, Suresh Babu S, Krishnamurthy S, Bhimaraj A, Youker KA, Kishore R, Krishnamurthy P. MicroRNA-9 inhibits hyperglycemia-induced pyroptosis in human ventricular cardiomyocytes by targeting ELAVL1. *Biochem Biophys Res Commun.* 2016;471:423-429.
27. Song Y, Yang L, Guo R, Lu N, Shi Y, Wang X. Long noncoding RNA MALAT1 promotes high glucose-induced human endothelial cells pyroptosis by affecting NLRP3 expression through competitively binding miR-22. *Biochem Biophys Res Commun.* 2019;509:359-366.
28. Wu M, Yang Z, Zhang C, Shi Y, Han W, Song S, Mu L, Du C, Shi Y. Inhibition of NLRP3 inflammasome ameliorates podocyte damage by suppressing lipid accumulation in diabetic nephropathy. *Metabolism.* 2021;118:154748.
29. Lee HM, Kim JJ, Kim HJ, Shong M, Ku BJ, Jo EK. Upregulated NLRP3 inflammasome activation in patients with type 2 diabetes. *Diabetes.* 2013;62:194-204.
30. Wang C, Pan Y, Zhang QY, Wang FM, Kong LD. Quercetin and allopurinol ameliorate kidney injury in STZ-treated rats with regulation of renal NLRP3 inflammasome activation and lipid accumulation. *PLoS One.* 2012;7:e38285.
31. Lu L, Lu Q, Chen W, Li J, Li C, Zheng Z. Vitamin D_3 protects against diabetic retinopathy by inhibiting high-glucose-induced activation of the ROS/TXNIP/NLRP3 inflammasome pathway. *J Diabetes Res.* 2018;2018:8193523.
32. Yang WH, Park SY, Nam HW, Kim DH, Kang JG, Kang ES, Kim YS, Lee HC, Kim KS, Cho JW. NFkappaB activation is associated with its O-GlcNAcylation state under hyperglycemic conditions. *Proc Natl Acad Sci U S A.* 2008;105:17345-17350.
33. Wellen KE, Hotamisligil GS. Inflammation, stress, and diabetes. *J*

Clin Invest. 2005;115:1111-1119.
34. Milanski M, Degasperi G, Coope A, Morari J, Denis R, Cintra DE, Tsukumo DM, Anhe G, Amaral ME, Takahashi HK, Curi R, Oliveira HC, Carvalheira JB, Bordin S, Saad MJ, Velloso LA. Saturated fatty acids produce an inflammatory response predominantly through the activation of TLR4 signaling in hypothalamus: implications for the pathogenesis of obesity. *J Neurosci.* 2009;29:359-370.
35. Thaler JP, Schwartz MW. Minireview: Inflammation and obesity pathogenesis: the hypothalamus heats up. *Endocrinology.* 2010;151:4109-4115.
36. Swisa A, Glaser B, Dor Y. Metabolic stress and compromised identity of pancreatic beta cells. *Front Genet.* 2017;8:21.
37. Guthrie RA, Guthrie DW. Pathophysiology of diabetes mellitus. *Crit Care Nurs Q.* 2004;27:113-125.
38. Galicia-Garcia U, Benito-Vicente A, Jebari S, Larrea-Sebal A, Siddiqi H, Uribe KB, Ostolaza H, Martín C. Pathophysiology of type 2 diabetes mellitus. *Int J Mol Sci.* 2020;21:6275.
39. Liang J, Chang B, Huang M, Huang W, Ma W, Liu Y, Tai W, Long Y, Lu Y. Oxymatrine prevents synovial inflammation and migration via blocking NF-κB activation in rheumatoid fibroblast-like synoviocytes. *Int Immunopharmacol.* 2018;55:105-111.
40. Liang L, Wu J, Luo J, Wang L, Chen ZX, Han CL, Gan TQ, Huang JA, Cai ZW. Oxymatrine reverses 5-fluorouracil resistance by inhibition of colon cancer cell epithelial-mesenchymal transition and NF-κB signaling *in vitro*. *Oncol Lett.* 2020;19:519-526.
41. Jiang G, Liu X, Wang M, Chen H, Chen Z, Qiu T. Oxymatrine ameliorates renal ischemia-reperfusion injury from oxidative stress through Nrf2/HO-1 pathway. *Acta Cir Bras.* 2015;30:422-429.
42. Li L, Liu Q, Fan L, Xiao W, Zhao L, Wang Y, Ye W, Lan F, Jia B, Feng H, Zhou C, Yue X, Xing G, Wang T. Protective effects of oxymatrine against arsenic trioxide-induced liver injury. *Oncotarget.* 2017;8:12792-12799.
43. Li M, Zhang X, Cui L, Yang R, Wang L, Liu L, Du W. The neuroprotection of oxymatrine in cerebral ischemia/reperfusion is related to nuclear factor erythroid 2-related factor 2 (nrf2)-mediated antioxidant response: role of nrf2 and hemeoxygenase-1 expression. *Biol Pharm Bull.* 2011;34:595-601.
44. Xu J, Li C, Li Z, Yang C, Lei L, Ren W, Su Y, Chen C. Protective effects of oxymatrine against lipopolysaccharide/D-galactosamine-induced acute liver failure through oxidative damage, via activation of Nrf2/HO-1 and modulation of inflammatory TLR4-signaling pathways. *Mol Med Rep.* 2018;17:1907-1912.